

Synthesis, Thermal Analysis, and Thermodynamic Properties Study of New Quinoline Derivative and Their V(IV), Co(II), and Cu(II) Complexes

Raghad Jawad Kadhim Aldoghachi¹, Faris Abdulridha Jassim Aldoghachi^{2*}, Tahseen Abdul Qader Alsalm³, and Mohd Lokman Ibrahim⁴

¹Department of Pharmaceutical Chemistry, University of Basrah, 61004, Basrah, Iraq

²Department of Chemistry, Faculty of Science, University of Basrah, 61004, Basrah, Iraq

³Department of Chemistry, Faculty of Education, University of Basrah, 61004, Basrah, Iraq

⁴School of Chemistry and Environment, Faculty of Applied Sciences, Universiti Teknologi MARA, Shah Alam, Selangor 40450, Malaysia

* Corresponding author:

tel: +964-780-0995900

email: farisj63@gmail.com

Received: April 28, 2022

Accepted: June 29, 2022

DOI: 10.22146/ijc.74423

Abstract: A new ligand (E)-2-((2-chloro-6-methylquinoline-3-yl)methylene)-N'-((E)-(2-chloro-6-methylquinoline-3-yl)methylene)hydrazine-1-carbothiohydrazide (QH) was prepared by reacting hydrazine hydrate with carbon disulfide to yield thiocarbohydrazide. The thiocarbohydrazide in the second step was treated with a quinoline derivative 2-chloro-6-methylquinoline-3-carbaldehyde to yield the ligand. The ligand was identified by spectroscopic techniques FTIR, ¹H-NMR, and ¹³C-NMR. Next, vanadium (V), cobalt (Co), and copper (Cu) complexes were prepared in the [M:L] ratio of 1:1 (QV, QCo, QCu). The complexes were characterized using FTIR, ESI, magnetic susceptibility, and molar conductivity. The thermal analysis (TGA) of V(IV), Co(II), and Cu(II) complexes were studied. The activation thermodynamic parameters, such as the energy of activation, enthalpy, entropy, and free energy change of the complexes, were evaluated, and the stabilities of the thermal decomposition of the complexes were discussed.

Keywords: quinoline derivative; thiocarbohydrazide; metal complexes; thermodynamic parameters

■ INTRODUCTION

Thiocarbohydrazide, H₂N-NH-(C=S)-NH-NH₂, is a promising unit for synthesizing new polyfunctional organic compounds following condensation with a ketone or an aldehyde. Both hydrazine groups of thiocarbohydrazide are very reactive and predominantly form bis-derivatives with aldehydes and ketones [1]. Although ligands with donor atoms, nitrogen, and oxygen, are by far the most thoroughly studied, interest in sulfur donor chelating agents has grown over time, and chemical studies in this area have increased significantly [2]. The coordination of a metal cation with a prepared ligand indicates that it has two azomethine nitrogen as donor atoms, which are the two terminal nitrogen atoms and, in most cases, the sulfur donor atom [3-4]. Interest

in these ligand system complexes now includes numerous areas, ranging from general considerations of the effect of sulfur and electron delocalization in transition metal complexes to potential biological activity and practical application [5-7].

Thiocarbohydrazones are a class of vital compounds in the pharmaceutical and medical fields. They possess several biological activities based on their parent aldehyde or ketone moiety. Among their biological activities are antibacterial, anticancer, antifungal, anti-inflammatory, antimycobacterial, antioxidative, antituberculosis, and herbicidal activities. Furthermore, thiocarbohydrazones are utilized as starting materials in the synthesis of industrial and biological compounds with the potential of developing a new class of antileishmanial compounds

[8-10]. The fungicidal activity of thiocarbohydrazones has been tested on textile fabrics [11], and recently, the synthesis and investigation of a series of 2-acetylpyridine thiocarbohydrazones as inactivators of Herpes simplex virus-1 (HSV-1) ribonucleotide reductase showed better results compared to analogous 2-acetylpyridine thiosemicarbazone derivatives [12]. The antifungal and antimicrobial properties of thiosemicarbazones and their transition metal complexes have been studied widely. However, little is known about the biological properties of thiocarbohydrazones [13]. Hence, the purpose of the present work was to synthesize a new thiocarbohydrazone ligand and determine its transition metal complexes with V(IV), Co(II), and Cu(II) ions that can potentially function as an antiviral agent.

■ EXPERIMENTAL SECTION

Materials

The *o*-aminophenol, chloroform, sulfuric acid, and *p*-toluidine were purchased from BDH, UK. Dimethylformamide, cyclohexane, diethyl ether, ethanol, hexane sulfuric acid, and glacial acetic acid were purchased from Sigma-Aldrich, Germany. Carbon disulfide, vanadyl sulfate pentahydrate, acetic anhydride, 4-bromoaniline, copper dichloride hexahydrate, cobalt dichloride, and hexahydrate were purchased from Fluka, Switzerland. Hydrazine and phosphoryl chloride were purchased from Merck, Germany. Acetone and dioxane were purchased from Fischer, UK. All materials and reagents were used without further purification, following the manufacturer's protocol.

Instrumentation

The studied compounds' infrared spectra were measured using FTIR spectrophotometer model FTIR Affinity 1, as KBr disks at room temperature and a range of 4000–400 cm^{-1} . ^1H -NMR spectra of the studied compounds were scanned on a Bruker Vance 500 MHz spectrometer, whereas the ^{13}C -NMR spectra were scanned on 125 MHz. TMS, as the internal standard, was used as a reference to determine the 0.0 ppm. DMSO- d_6 was used as a solvent.

TGA studies were conducted using Mettler Toledo

with a 10 $^\circ\text{C}/\text{min}$ heat rate and a range of 0–700 $^\circ\text{C}$. The Electrospray Ionization (ESI) of the compounds was measured by Waters Alliance 2695 HPLC-Micromass Quattro micro-API Mass Spectrometer.

The magnetic susceptibility of the complexes was measured at room temperature using the Gouy Method Model with a device manufactured from Auto Magnetic Susceptibility (Sherwood scientific). The correction factor for the prepared complexes was calculated using Pascal's constants for the atoms constituting the complexes. The molar conductivity of the complexes was measured using a conductivity device manufactured by a Switzerland company at a temperature of 25 $^\circ\text{C}$ using dimethylformamide (DMF) as a solvent at 1×10^{-3} M.

Procedure Preparation of the Ligand (QH)

Preparation of thiocarbohydrazone

Thiocarbohydrazone was prepared by adding (0.5 mol, 24 mL) of hydrazine hydrate to (75 mL) of distilled water in a flask. Next, (0.25 mol, 15 mL) of carbon bisulfide was added dropwise with continuous stirring for 1 h at room temperature. The mixture was then heated for 2 h, cooled in an ice bath, and filtered. The precipitate was recrystallized from water, with a yield of 95% (0.836 g), m.p. (171–174 $^\circ\text{C}$) [14].

Synthesis of the ligand (E)-2-((2-chloro-6-methylquinoline-3-yl)methylene)-N'-((E)-(2-chloro-6-methylquinoline-3-yl)methylene)hydrazine-1-carbothiohydrazone (QH)

2-Chloro-6-methylquinoline-3-carbaldehyde (2.5 mmol) 0.5 g and (1 mmol) 0.106 g thiocarbohydrazone were mixed in a round flask with 10 mL ethanol and a few drops of acetic acid as catalyst. The mixture was heated with reflux for 2 h, and the reaction mixture was monitored by TLC using ethanol: chloroform (2:8 v/v). The mixture was cooled, filtered, dried, and recrystallized from dioxane [15]. The pale yellow powder was obtained with a yield of 75 % (0.879 g) m.p. (190–193 $^\circ\text{C}$).

Synthesis of the complexes

Vanadyl complex: Diaqua [((E)-2-((2-chloro-6-methylquinoline-3-yl)methylene)-N'-((E)-(2-chloro-6-methylquinoline-3-yl)methylene)hydrazine-1-carbothiohydrazone)

Vanadium(IV) chloride] (QV). The vanadyl complex was prepared by reacting (1 mmol, 0.18 g) $\text{VO}_2\text{Cl}_2 \cdot 2\text{H}_2\text{O}$ and (1 mmol, 0.481 g) of the ligand (QH) with 50 mL of dioxane followed by 2 h reflux to obtain the vanadyl complex QV filtrate. The filtrate was then washed twice with diethyl ether and dioxane to produce a dried brown powder with a yield of 90% (0.589 g).

Cobalt complex: Tetra-aqua ((E)-2-((2-chloro-6-methylquinoline-3-yl)methylene)-N'-(E)-(2-chloro-6-methylquinoline-3-yl)methylene)hydrazine-1-carbothiohydrazide) Cobalt(II) chloride (QCo). Cobalt complex was prepared by reacting (1 mmol, 0.237 g) cobalt chloride, $\text{CoCl}_2 \cdot 6\text{H}_2\text{O}$, and (1 mmol, 0.481 g) ligand (QH) with 50 mL Dioxane and reflux for 2 h to yield brown powder cobalt complex, the yield of 98% (0.670 g).

Copper complex: Diaqua ((E)-2-((2-chloro-6-methylquinoline-3-yl)methylene)-N'-(E)-(2-chloro-6-methylquinoline-3-yl)methylene)hydrazine-1-carbothiohydrazide) Copper(II) chloride (QCu). The copper complex was prepared by reacting (1 mmol, 0.170 g) of copper chloride, $\text{CuCl}_2 \cdot 2\text{H}_2\text{O}$, and (1 mmol, 0.481 g) of ligand (QH) with 50 mL dioxane and reflux for 2 h to yield dark green powder, the yield of 95% (0.618 g)

m.p. dec. < 250 °C. Table 1 lists the physical properties of the new complexes.

RESULTS AND DISCUSSION

The present study focused on the synthesis of transition metal complexes V(IV), Co(II), and Cu(II) with the ligand QH (Fig. 1). Scheme 1 demonstrates the synthesis path of ligand QH.

FTIR Spectra of the Complex (QV, QCo, and QCu)

The IR spectrum of the ligand (QH) displays the H-N group's stretching vibration band at 3450 cm^{-1} and stretching bands at 3051 and 2954 cm^{-1} , attributed to the aromatic and aliphatic C-H, respectively. The appearance of the stretching band at 1691 cm^{-1} was due to azomethine C=N. The band at wavenumber 1581 cm^{-1} was attributed to the stretching vibration of the aromatic C=C, whereas the band at 1303 cm^{-1} was due to the bending vibration of the C-N group. The band at 1176 cm^{-1} was attributed to C=S, as displayed in Table 2.

The FTIR spectra of the studied complexes are shown in Fig. 2, and the data is in Table 2. All the spectra

Table 1. Physical properties of the new complexes

Complex	Molecular formula	M.wt (g/mol)	Color	Yield (%)
QH	$\text{C}_{23}\text{H}_{18}\text{Cl}_2\text{N}_6\text{S}$	481.40	Yellow pale	75
QV	$\text{C}_{23}\text{H}_{18}\text{Cl}_2\text{N}_6\text{SV}$	655	Brown	90
QCo	$\text{C}_{23}\text{H}_{20}\text{Cl}_2\text{CoN}_6\text{O}_2\text{S}$	684	Brown	98
QCu	$\text{C}_{23}\text{H}_{18}\text{Cl}_2\text{CuN}_6\text{S}$	651	Dark green	95

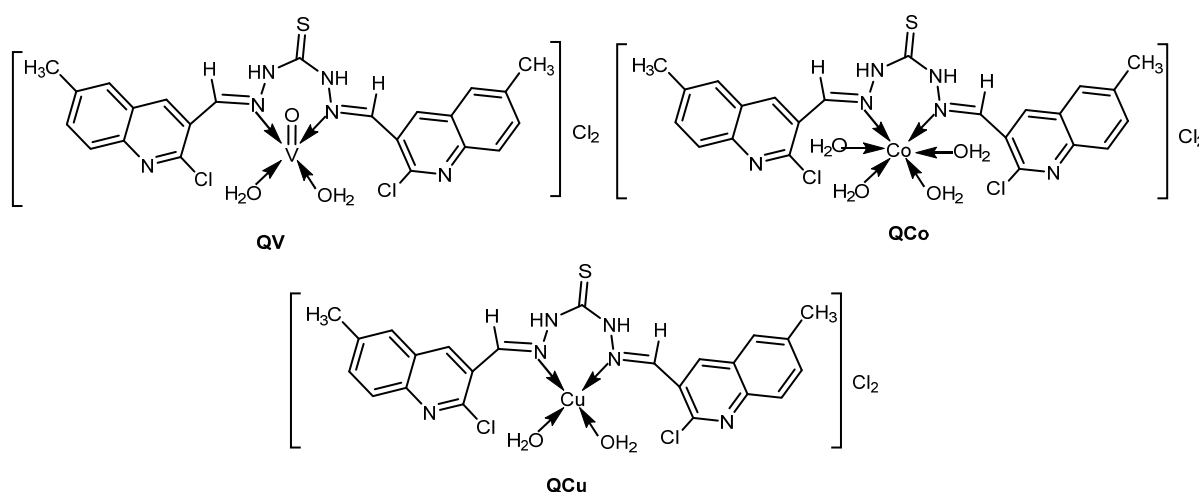
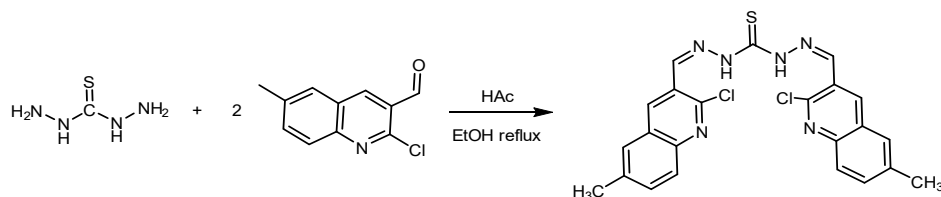


Fig 1. Structure of complexes QV, QCo, and QCu



Scheme 1. The synthesis path of ligand OH

Table 2. IR spectra data of the complexes

Complex	Stretching									
	O-H	N-H	Ar-H	C-H	C=N	C=C	C-N	C=S	C-Cl	Other
QH	-----	3450	3051	2922	1691	1581	1303	1176	736	-----
QCu	3446	3358	3053	2926	1620	1558	1375	1195	823	N-Cu 561
QV	3421	3344	3051	2921	1614	1554	1333	1265	761	N-V 522
QCo	3400	3261	3060	2902	1656	1566	1377	1220	750	N-Co 550

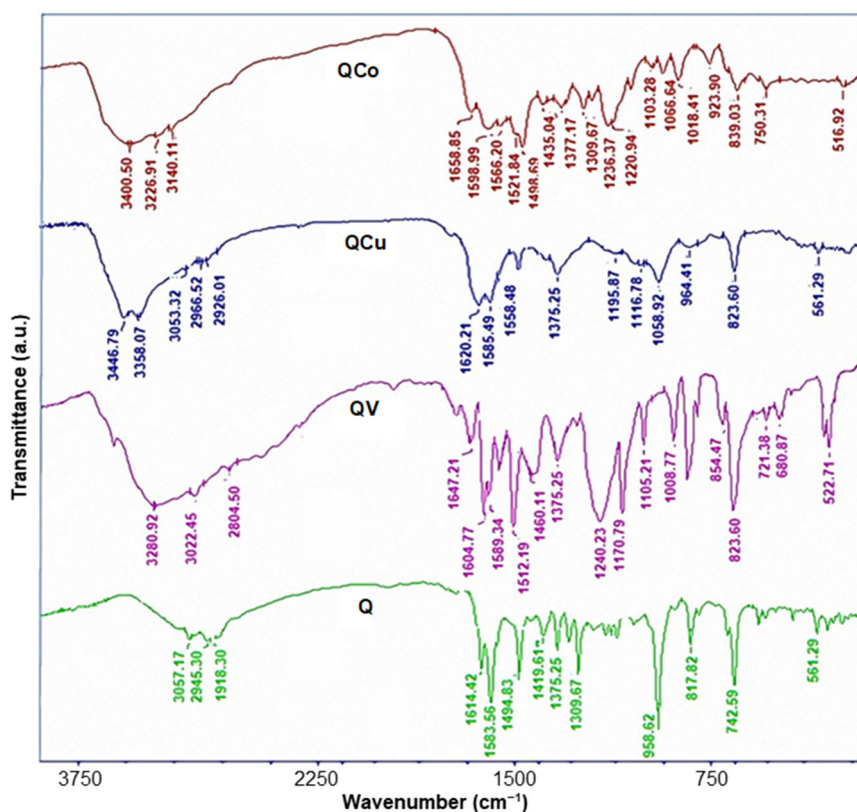


Fig 2. FTIR spectra of the ligands and their complexes

displayed bands of stretching vibration of the O-H group within the range of 3400–3446 cm^{-1} , whereas the bands of stretching vibration of the N-H group were observed in the region of 3261–3358 cm^{-1} . The stretching vibration band of the Ar C-H group was seen within the range of 3053–3060 cm^{-1} . Whereas those in the range of 2902–2926 cm^{-1} were due to the aliphatic C-H group. The bands

related to the C=N group were observed in 1614–1656 cm^{-1} . The IR spectrum of all complexes showed bands of stretching vibration of the C=C group within the range of 1554–1566 cm^{-1} , whereas the bands of C-N stretching vibration were seen in the range of 1333–1377 cm^{-1} . The bands related to the C=S group were observed in the range of 1195–1265 cm^{-1} , and the bands

of stretching vibration within the region of 750–823 cm^{-1} were attributed to the C-Cl group. As for the bonding of the ligands with transition metals, the bands showed a stretching vibration in the region of 522–561 cm^{-1} [16–17]. However, no broad band of stretching vibration of the O-H group was observed for the ligand QH, indicating the formation of complexes.

$^1\text{H-NMR}$ and $^{13}\text{C-NMR}$ Spectrum of QH

The $^1\text{H-NMR}$ spectra of the synthesized ligand were recorded on a Bruker Avance 500 MHz spectrometer used to confirm the proposed structure of QH in $\text{DMSO-}d_6$, with tetramethylsilane (TMS) as the internal standard. The peaks at 2.5 and 3.3 ppm were attributed to DMSO and water solution, respectively [18]. The main peaks appear in Table 3 (Supplementary Fig. S1).

The $^{13}\text{C-NMR}$ spectrum of the new compound data is summarized in Table 4 (Supplementary Fig. S2). The spectra showed a heptate signal at 39 ppm due to the $\text{DMSO-}d_6$ solvent [19].

Magnetic Susceptibility

Magnetic susceptibility is one of the methods for single electrons used to study the complex's properties. Paramagnetic properties are obtained when the central

atom contains single electrons, whereas diamagnetic properties are obtained when double electrons are present. This method is successfully implemented for studying the complex's geometry, shape, hybridization, and oxidation number [20].

The magnetic properties of complexes are due to the orbital and perchance motion. The theoretical magnetic moment of the first transition series of metal ions is defined by the following equation (Eq. (1)):

$$\mu = \sqrt{4S(S+1) + (L+1)B.M} \quad (1)$$

Most of the paramagnetic materials consist of paramagnetic centers and diamagnetic groups. Hence, the obtained values for the magnetic susceptibility need to be corrected based on Pascal's constants to calculate the value of the correction factor (D) and reduce the error rate arising from the magnetic influences.

In this study, we relied on Faraday's method for forbidden complexes and the magnetic moment values were calculated based on the following equations:

$$\begin{aligned} \mu_{\text{eff}} &= 2.82 \times (X_A \times T)^{1/2} \\ X_A &= X_m - (-D) \\ X_m &= X_g * M \end{aligned} \quad (2)$$

where X_g : weight susceptibility, M: molecular weight of the complex, X_m : molar susceptibility, X_A : atom's susceptibility,

Table 3. The $^1\text{H-NMR}$ data of the ligand QH

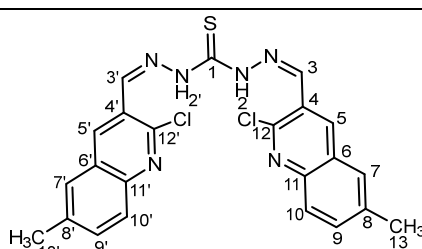
Structure	Chemical shift (ppm)
	(13.13') 2.43 (s, 6H, CH_3)
	(10.10') 7.30 (d, 2H, Ar-H)
	(9.9') 7.72 (d, 2H, Ar-H)
	(5.5') 7.80 (s, 2H, Ar-H)
	(7.7') 8.08 (s, 2H, Ar-H)
	(3.3') 8.64 (s, 2H, $\text{CH}=\text{N}$)
	(2.2') 10.96 (s, 2H, N-H)

Table 4. The $^{13}\text{C-NMR}$ data of the ligand QH

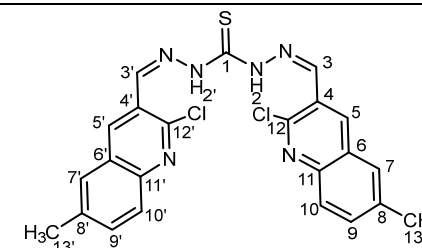
Structure	Chemical shift (ppm)
	169.3: C=N (C3, C3')
	151-149: C=N ring
	143-141: C-Cl (C12, C12')
	134-121: Aromatic carbon
	21.06: CH_3 , (C13, C13')

Table 5. Magnetic properties of the prepared complexes

Complex	$X_g \cdot 10^{-4}$	X_M	X_A	$D \cdot 10^{-6}$	μ_{eff} B.M
QCo	0.099	0.0067617	0.00692425	-162.65	4.09
QCu	0.018	0.001178	0.00130836	-136.56	1.78
QV	0.021	0.0013755	0.00151206	-136.56	1.9

D: diamagnetic correction, μ_{eff} : effective magnetic momentum, T: absolute temperature, X_g : given from the device by the practical measurement of the solid model

The magnetic moment calculated for the QCo was 4.09 M.B (Table 5), indicating a paramagnetic character due to the presence of three single electrons in the outer shell. The geometrical shape was octahedral due to the sp^3d^2 hybridization [21]. The complexes, QV and QCu, had a paramagnetic character due to the presence of one single electron in the outer shell. The value of the magnetic moment of the QCu demonstrated that the geometrical shape of the complex was a square planer due to the dsp^2 hybridization, while based on the value obtained for the QV, the geometrical shape was square pyramidal due to the dsp^3 hybridization [22].

Molar Conductivity

Molar conductivity is extensively used in the field of coordination chemistry to investigate the ionic formula of compounds in the solution when in the solid-state [23]. The greater number of ions released by the complex in the solution, the higher degree of molar conductivity. The complexes with low molar conductivity due to difficult ionization can be neglected. and can be calculated the conductivity by using the following relationship

$$\Lambda_m = \Lambda_\infty - K_c C^{1/2} (\text{mol}^{-1} \cdot \text{cm}^2 \cdot \Omega^{-1}) \quad (3)$$

Λ_m : molar conductivity, Λ_∞ : electrical conductivity at the final dilution

$$\Lambda = 10^3 K_c / C \quad (4)$$

Therefore, based on the values presented in Table 6, it was concluded that the solutions were electrolytes.

The Electrospray Ionization (ESI)

The soft ionization mass spectrum is a valuable instrument for obtaining the molecular structure of the molecules by the appearance of a molecular ion signal

Table 6. Molar conductivity of the complexes

Complex	Molar conductivity ($\text{mol}^{-1} \cdot \text{cm}^2 \cdot \Omega^{-1}$)
QCo	140.8
QCu	93.38
QV	132.6

corresponding to the compound's molecular weight. The spectra data can be seen in Table 7 (Supplementary Fig. S3-5). The protonation ion of the analyst $[M+H]^+$ can normally be used to identify the molecular weight of the compound. Although fragmentation is possible due to ESI-MS experimental conditions, it yields less intense fragment ion peaks as compared to electron impact (EI). The ESI mass spectra of complexes gave a molecular ion peak equal to $[M+1]^+$. The mass spectra confirmed the proposed chemical structure of these complexes. As can be observed in Table 7, the molecular weight of QCo was 683, while the $[M+H]^+$ was 684. The molecular weight of the QCu was 651, while the $[M+H]^+$ was 652. The molecular weight of the QV was 655, while the $[M+H]^+$ was 656.

Thermal Analysis

Thermal analysis (TG and DTG) was utilized to determine the thermal stability of these complexes and to confirm whether water molecules were inside or outside the central metal ion's inner coordination sphere. The complexes were heated to 700 °C in a nitrogen environment at a rate of 10 °C/min for TG analysis. The mass losses calculated using TG curves were very close to the calculated values. All complex degradation paths, which differ from one to the next, confirm the postulated structures [7].

Table 8 represents the thermal breakdown data of the complexes and reveals that the complexes' remaining components were more stable [24]. The thermal curve of the QCo at the first stage of 90–150 °C represents the loss of water of crystallization molecules with a practical loss

Table 7. The ESI of the complexes

Complex	Structure	M.wt	[M+H] ⁺
QV		655	656
QCo		683	684
QCu		651	652

Table 8. Thermogravimetric analysis of the prepared complexes

Complex	Decom. temp. (°C)			Char. content at 600 °C	Mass loss (%) theoretical	Assignment
	T _i	T _{max}	T _f			
QCo	90	133	150	38.35%	10.5 (10.7)	H ₂ O crystallization
	150	300	320		10.5 (10.6)	4H ₂ O coordination
	320	420	600		40.35	Survival of parts of the ligand
QCu	100	140	170	55.84%	5.5 (5.51)	H ₂ O crystallization
	170	220	270		11 (10.4)	2H ₂ O coordination
	270	300	600		25.15	Survival of parts of the ligand
QV	90	130	150	75.43%	5.49 (5.51)	H ₂ O crystallization
	150	305	350		10.98 (11.8)	2H ₂ O coordination
	350	470	600		7.26	Survival of parts of the ligand

of 10.7% and a theoretical ratio of 10.5% (DTG_{max} 133 °C). As for the second stage of 150–320 °C, which represents the loss of four molecules of coordinated water (4H₂O), the percentage of practical loss was 10.6%, the theoretical percentage was 10.5%, and the DTG_{max} was at 300 °C. As for the third stage, which appears clearly in the spectrum of TG, DTG at 320–600 °C, the results revealed loss of parts of the ligand with a percentage of 40.35%, and the residual percentage was 38.35%, indicating the survival of parts of the ligand at the end of the stage, which exceeds the proportion of cobalt oxide (CoO) with a theoretical

ratio of 10.9%. The results show that the complex has high thermal stability and intensity of bonding of the ligand with the metal (Supplementary Fig. S6).

As for the QCu, the thermal analysis curve demonstrates several stages of loss. The first stage is represented by 100–170 °C (DTG_{max} 140 °C), demonstrating a practical loss of 5.51% and a theoretical ratio of 5.5% (loss of crystallization water molecules). As for the second stage of 170–270 °C (DTG_{max} 220 °C), the results revealed the loss of two molecules of coordinated water (2H₂O), and the third stage of 270–600 °C

(DTG_{max} 300 °C) showed the loss of parts of the ligand with a percentage of loss of 25.15% and a residual percentage of 55.84%. This percentage exceeds the percentage of copper oxide (CuO) as we relate it to the theory (12.1%), and this explains the presence of organic parts of the ligand connected to the metal (Supplementary Fig. S7).

With regards to the QV, the thermal curve of the complex where the first stage starts from 90–150 °C (DTG_{max} 130 °C) represents the loss of a molecule of crystallization water (H₂O), whereby the practical loss ratio was 5.51%, and the theoretical ratio was 5.49%. At the second stage of 150–350 °C (DTG_{max} 305 °C), the practical loss ratio was 11.8%, and the theoretical ratio was 10.98%, representing the loss of a molecule of coordinated water (2H₂O). Furthermore, the third stage was clear in the spectrum (TG, DTG) at 350–600 °C (DTG_{max} 470 °C) due to the loss of parts of ligand at a percentage of 7.26% with a residual ratio of 75.43%, indicating the survival of parts of the ligand at the end of the process which exceeded the percentage of vanadium oxide (VO₂) (theoretical part of 12.28%). This is explained by the fact that the complex has thermal stability and strong bonding of the ligand with the metal (Supplementary Fig. S8).

In summary, it is evident that the shapes of the proposed complexes were accurately correct, as demonstrated in the analyzed results. The mass spectrum revealed the proposed molecular weight of each complex, and the thermal analysis of the complexes demonstrated that they contain water of coordination, both according to their composition. Also, the molar conductivity showed that the complexes were ionic due to the presence of chlorine ions outside of the coordination sphere. The

study of the magnetic susceptibility showed the hybridization and geometrical shapes of the molecules through the number of single electrons for each metal ion.

Calculation of the Thermodynamic Functions of the Prepared Complexes

The thermodynamic functions of the complexes prepared in this study were calculated in a range of different temperatures of 150–600 °C (Table 9). The data indicate a gradual increase in the values of stability constants at higher temperatures. The increase in the values of the stability constants in this study with the increase in temperature enabled us to study this interaction from a thermodynamic point of view, i.e., extracting the thermodynamic variables, each of which has a change in enthalpy (ΔH), a change in free energy (ΔG), and a change in entropy (ΔS), from the Coats-Redfern equation at all the temperatures mentioned above, represented by the Eq. (5) [25]:

$$\log \left[\frac{\log \frac{W_f}{W_f - W_t}}{T^2} \right] = \log \left[\frac{AR}{\theta E} \left(1 - \frac{2RT}{E} \right) \right] - \frac{E}{2.303RT} \quad (5)$$

where, W_f = weight loss at the end of stage; W_t = weight loss at temp (t); E = activation energy; A = constant; θ = constant; R = gas constant = 8.314 M⁻¹.J⁻¹.K; T = absolute temperature.

$$\Delta G = \Delta H - T\Delta S \quad (6)$$

After calculating the thermodynamic functions based on the above equation, what follows is evident. The negative ΔS values meant that all the processes took place at a low rate and that the activated complex was more ordered than either of the reactants. Furthermore,

Table 9. Kinetic parameters of the complexes using the Coats–Redfern equation

Complex	Stage	A (s ⁻¹)	E (kJ.mol ⁻¹)	ΔH (kJ.mol ⁻¹)	ΔS (kJ.mol ⁻¹ .K ⁻¹)	ΔG (kJ.mol ⁻¹)
QCo	I	2.19 × 10 ⁴	6.25 × 10 ¹	59.12	-0.16	1.25 × 10 ⁵
	II	5.20 × 10 ¹³	1.52 × 10 ¹²	147.20	0.01	1.54 × 10 ²
QCu	I	2.18 × 10 ⁵	5.97 × 10 ¹	56.79	-0.14	1.06 × 10 ²
	II	7.21 × 10 ²²	1.20 × 10 ²	196.38	0.19	-1.18 × 10 ¹
	III	8.51 × 10 ⁹	1.19 × 10 ²	114.45	-0.06	1.44 × 10 ²
QVO	I	1.01 × 10 ⁶	1.80 × 10 ¹	13.16	-0.14	9.12 × 10 ¹
	II	1.00 × 10 ¹¹	1.98 × 10 ²	191.80	-0.04	2.23 × 10 ²

the values of ΔH of activation were positive for all the complexes, indicating the endothermic nature of the process. In addition, all the ΔG values were positive, demonstrating that all steps were nonspontaneous (Table 9).

■ CONCLUSION

We have synthesized new V(IV), Co(II), and Cu(II) complexes with quinoline-thiocarbohydrazide ligands containing different steric and electronic properties in good yields. The new complexes have been well-characterized by FTIR, $^1\text{H-NMR}$, $^{13}\text{C-NMR}$, ESI-MS, TGA, molar conductance, magnetic susceptibility, and calculating the thermodynamic function. The studied complexes were found to be more stable at 700 °C. Findings from this study provide insight into the potential role of the synthesized thiocarbohydrazone ligand and its transition metal complexes as potential virotherapy.

■ ACKNOWLEDGMENTS

We thank the University of Basrah for all the provided facilities.

■ AUTHOR CONTRIBUTIONS

Faris A.J. Aldoghachi and Tahseen A. Alsalmim were involved in supervision, funding provision, conceiving the experimental design of the study, and reviewing and editing the manuscript. Raghad J.K. Aldoghachi was involved in conducting the experiment, data collection and analysis, and writing the manuscript. Mohd Lokman Ibrahim was involved in the provision of resources, analysis, and revision of the paper.

■ REFERENCES

- [1] Kaya, Y., Erçağ, A., and Kaya, K., 2018, Synthesis, characterization and antioxidant activities of dioxomolybdenum(VI) complexes of new Schiff bases derived from substituted benzophenones, *J. Coord. Chem.*, 71 (20), 3364–3380.
- [2] Kareem, M.J., Al-Hamdani, A.A.S., Ko, Y.G., Al Zoubi, W., and Mohammed, S.G., 2021, Synthesis, characterization, and determination antioxidant activities for new Schiff base complexes derived from 2-(1H-indol-3-yl)-ethylamine and metal ion complexes, *J. Mol. Struct.*, 1231, 129669.
- [3] Burrows, A.D., Menzer, S., Mingos, D.M.P., White, A.J., and Williams, D.J., 1997, The influence of the chelate effect on supramolecular structure formation: Synthesis and crystal structures of zinc thiourea and thiosemicarbazide complexes with terephthalate, *J. Chem. Soc., Dalton Trans.*, 22, 4237–4240.
- [4] Shaalan, N., Khalaf, W.M., and Mahdi, S., 2022, Preparation and characterization of new tetradentate N_2O_2 Schiff base with some of metal ions complexes, *Indones. J. Chem.*, 22 (1), 62–71.
- [5] Al-Saadawy, N.H., 2022, Synthesis, characterization, and theoretical study of some new organotellurium compounds derived from camphor, *Indones. J. Chem.*, 22 (2), 437–445.
- [6] Al-Saadawy, N.H., 2021, Synthesis, characterization, and theoretical studies of new organotellurium compounds based on (4-(((1S,E)-1,7,7-trimethylbicyclo[2.2.1]heptan-2-ylidene)amino)phenyl)mercury(II) chloride, *Indones. J. Chem.*, 21 (6), 1443–1453.
- [7] Jirjees, V.Y., Al-Hamdani, A.A.S., Wannas, N.M., Farqad, A.R., Dib, A., and Al Zoubi, W., 2021, Spectroscopic characterization for new model from Schiff base and its complexes, *J. Phys. Org. Chem.*, 34 (4), e4169.
- [8] Božić, A.R., Bjelogrić, S.K., Novaković, I.T., Filipović, N.R., Petrović, P.M., Marinković, A.D., Todorović, T.R., and Cvijetić, I.N., 2018, Antimicrobial activity of thiocarbohydrazones: Experimental studies and alignment-independent 3D QSAR models, *ChemistrySelect*, 3 (7), 2215–2221.
- [9] Božić, A., Marinković, A., Bjelogrić, S., Todorović, T.R., Cvijetić, I.N., Novaković, I., Muller, C.D., and Filipović, N.R., 2016, Quinoline based mono- and bis-(thio)carbohydrazones: Synthesis, anticancer activity in 2D and 3D cancer and cancer stem cell models, *RSC Adv.*, 6 (106), 104763–104781.
- [10] Mojallal-Tabatabaei, Z., Foroumadi, P., Toolabi, M., Goli, F., Moghimi, S., Kaboudanian-Ardestani, S., and Foroumadi, A., 2019, 2-(Bipiperidin-1-yl)-

- 5-(nitroaryl)-1,3,4-thiadiazoles: Synthesis, evaluation of *in vitro* leishmanicidal activity, and mechanism of action, *Bioorg. Med. Chem.*, 27 (16), 3682–3691.
- [11] Neunhoeffer, H., and Wiley, P.F., 2009, *The Chemistry of Heterocyclic Compounds: Chemistry of 1,2,3-Triazines and 1,2,4-Triazines, Tetrazines, and Pentazin*, Vol. 33, Wiley-Interscience, Hoboken, US.
- [12] Obaid, S.M.H., Sultan, J.S., and Al-Hamdani, A.A.S., 2020, Synthesis, characterization and biological efficacies from some new dinuclear metal complexes for base 3-(3,4-dihydroxy-phenyl)-2-[(2-hydroxy-3-methylperoxy-benzylidene)-amino]-2-methyl propionic acid, *Indones. J. Chem.*, 20 (6), 1311–1322.
- [13] Shaalan, N., Abed, A.Y., Alkubaisi, H.M., and Mahde, S., 2019, Synthesis, spectroscopy, biological activities and thermodynamic studies for new complexes of some lanthanide metals with Schiff's bases derived from [2-acetylthiophene] with [2,5-dihydrazino-1,3,4-thiadiazole], *Res. J. Chem. Environ.*, 23, 181–187.
- [14] Shaalan, N.D., and Abdulwahhab, S.M., 2021, Synthesis, characterization and biological activity study of some new metal complexes with Schiff's bases derived from [*o*-vanillin] with [2-amino-5-(2-hydroxy-phenyl)-1,3,4-thiadiazole], *Egypt. J. Chem.*, 8 (8), 4059–4067.
- [15] Al-Obaidy, G., Ibraheem, K.R., and Mesher, M.F., 2020, Synthesis and characterization of some new Cu II, Co II, Ni II, Au III potassium 2-(2,4-dinitrophenyl) hydrazine-1-carbodithioate complexes and evaluation of their biological activity, *Int. J. Pharm. Res.*, 12 (1), 1025–1032.
- [16] Obaid, S.M.H., Jarad, A.J., and Al-Hamdani, A.A.S., 2020, Synthesis, characterization and biological activity of mixed ligand metal salts complexes with various ligands, *J. Phys.: Conf. Ser.*, 1660, 012028.
- [17] Abdalnabi, Z.A., Al-doghachi, F.A.J., and Abdulsahib, H.T., 2021, Synthesis, characterization and thermo gravimetric study of some metal complexes of selenazone ligand nanoparticles analogue of dithizone, *Indones. J. Chem.*, 21 (5), 1231–1243.
- [18] Deligeorgiev, T., Gadjev, N., Vasilev, A., Kaloyanova, S., Vaquero, J.J., and Alvarez-Builla, J., 2010, Green chemistry in organic synthesis, *Mini-Rev. Org. Chem.*, 7 (1), 44–53.
- [19] Jasim, A.M., 2011, Preparation and characterization of novel 3-(4-chloro phenyl)-1-nitro phenyl-5-(substituted phenyl)-formazans, *J. Basrah Res.*, 37 (5), 90–98.
- [20] Morrison, M.D., Hanthorn, J.J., and Pratt, D.A., 2009, Synthesis of pyrrolnitrin and related halogenated phenylpyrroles, *Org. Lett.*, 11 (5), 1051–1054.
- [21] Tiekink, E.R.T., 2018, Competing supramolecular interactions in crystals of heavy-element compounds—a consideration of the energies of association between molecules, *2nd Southeast Asian Conference on Crystal Engineering (SEACCE-2)*, Sunway University, Selangor, August 6-8th, 2018.
- [22] Alsalam, T.A., Hadi, J.S., Ali, O.N., Abbo, H.S., and Titinchi, S.J.J., 2013, Oxidation of benzoin catalyzed by oxovanadium (IV) Schiff base complexes, *Chem. Cent. J.*, 7 (1), 3.
- [23] Zajdel, P., Partyka, A., Marciniak, K., Bojarski, A.J., Pawlowski, M., and Wesolowska, A., 2014, Quinoline- and isoquinoline-sulfonamide analogs of aripiprazole: Novel antipsychotic agents?, *Future Med. Chem.*, 6 (1), 57–75.
- [24] Shim, J.O., Jeong, D.W., Jang, W.J., Jeon, K.W., Jeon, B.H., Kim, S.H., Roh, H.S., Na, J.G., Han, S.S., and Ko, C.H., 2016, Bio-diesel production from deoxygenation reaction over Ce_{0.6}Zr_{0.4}O₂ supported transition metal (Ni, Cu, Co, and Mo) catalysts, *J. Nanosci. Nanotechnol.*, 16 (5), 4587–4592.
- [25] Ebrahimi, H.P., Hadi, J.S., Abdalnabi, Z.A., and Bolandnazar, Z., 2014, Spectroscopic, thermal analysis and DFT computational studies of salen-type Schiff base complexes, *Spectrochim. Acta, Part A*, 117, 485–492.